J. Phys. Chem. A **2002,** *106,* 8917−8924

Theoretical Study on Potential Energy Surface of the C_2H_2FO Radical

Dong-bo Cao,* Yi-hong Ding, Ze-sheng Li, Xu-ri Huang, and Chia-chung Sun

State Key Laboratory of Theoretical and Computational Chemistry, Institute of Theoretical Chemistry, Jilin University, Changchun 130023, People's Republic of China

Received: November 29, 2001; In Final Form: May 28, 2002

The potential energy surface of C_2H_2FO is investigated at CCSD(T)/6-311G(d,p)//B3LYP/6-311G(d,p) level. The results show that isomers of 1, 3, 4, 5, 5′, 8, 9, and 9′ are stable, and the energy barriers are more than 30 kcal/mol. Isomer 2 has, relatively speaking, much lower kinetic stability. The three cyclic isomers 6, 6′, and 7 are less stable than the former, but more stable than the latter. The other isomers, such as isomers 1′, 3′, 4′, 10, and 11 are less stable than isomer 2 in kinetics. Only isomer 1 was synthesized experimentally, and the calculated frequencies are in good agreement with experimental values, so we conjecture that in the future, other stable isomers may be synthesized by the experimental methods, for example, coming from such reactions as FCCH + OH, CH_2F + CO, and so forth. Compared to the analogous C_2H_3O radical isomers, the energy order is changed. This may be due to conjugation of the carbonyl group in isomer 1 CH_2CFO with the substituent fluorine at the α-position.

1. Introduction

The fluorinated analogue of the vinoxy radical C_2H_2FO plays a significant role in atmospheric chemistry. This is because the C_2H_2FO radical is an important intermediate of the photochemistry reactions:[1] $CH_2CHF + O(^3P)$, $CH_2CF_2 + O(^3P)$, and $CH_2CFCl + O(^3P)$, which are harmful to stratospheric ozone, terrestrial ecosystems, and groundwater supplies.[2,3] An understanding of the role of C_2H_2FO radical in the photochemistry is critical to monitor waste remediation efforts and model atmospheric ozone depletion.[4]

The analogous vinoxy radical plays a major role in the gasphase oxidation of unsaturated hydrocarbons[5] and is an important intermediate in combustion[6] and photochemical smog cycles.[7] And C_2H_3O radical is interesting because it has two electronic states in the ground state, and both experiment[8] and ab initio calculations[9−13] have confirmed that fact. No experimental and theoretical investigation has been done on the electronic states of the fluorinated analogue of the vinoxy radical. In 1997, the C_2H_2FO radical was observed by laser-induced fluorescence spectrum, and theoretical calculation of three planar isomers confirmed that the most stable isomer ($CH_2CF{=}O$) was produced.[1] In 1999, the isotope C_2D_2FO radical was synthesized with the similar experiments.[14]Another reaction of F + CH_3COCl was studied by the infrared chemiluminescence method in flow reactor in 1998,[15] and it suggests that CH_2FCO intermediate is easily dissociated to CH_2F + CO, which is in agreement with the calculations in this paper. The α- and β-position of the substituent effect about the reaction of $R(R{=}H, CH_3, OH, F, SiH_3, Cl) + CH_2{=}C{=}O \rightarrow RCH_2C{=}O$, $CH_2(C{=}O)R$, $CH_2{=}COR$ was theoretically analyzed.[16] For the C_2H_2FO radical, only two isomers of $CH_2CF{=}O$ and CH_2FCO, and one transition state, were considered. In these studies, many other isomers were not synthesized experimentally and instead theoretically studied. Thus, in this paper, we focus on a detailed theoretical study for the potential energy surface of C_2H_2FO radical. Many isomeric structures and interconversion transition states are considered, including the analysis of dipole moment, infrared intensity, and rotational constant. We want to resolve the following questions: (1) What are the differences and similarities between C_2H_2FO and C_2H_3O radical? (2) How does the fluorine substituent affect the kinetic stability of C_2H_2FO radical?

2. Computational Methods

All of the calculations were carried out using the Gaussian 98 program package. The geometries of stationary points including minima isomers, transition states, and dissociated products were calculated by means of ab initio methods, including the density functional theory (DFT), Beck's three parameter hybrid methods with the Lee−Yang−Parr correlation functional (B3LYP), and the coupled cluster calculation with singles and doubles (CCSD), as well as with triples [CCSD(T)]. Single-point CCSD(T)/6-311G(d,p) calculations were carried out at the B3LYP/6-311G(d.p) geometries. The stationary nature of various structures was confirmed by harmonic vibration frequency calculations. Isomers possess all real frequencies, whereas transition states possess one and only one imaginary frequency. To test whether the obtained transition states connect the right isomers, the intrinsic reaction coordinate (IRC) calculations were performed at the B3LYP/6-311G(d,p) level.

3. Results and Discussions

Seventeen isomeric structures of C_2H_2FO radical are optimized and 30 interconversion transition states are obtained at B3LYP/6-311G(d,p) level. The structures of C_2H_2FO intermediate isomers are shown in Figure 1. The structures of interconversion transition states are depicted in Figure 2. The harmonic vibrational frequencies, as well as the infrared intensities, dipole moments, and rotational constants of the C_2H_2FO, are listed in Table 1, whereas the frequencies and intensities of all transition states are given in Table 2. The total and relative energies of all energy minima and transition states are collected in Table 3. Finally, a schematic potential energy surface (PES) of C_2H_2FO showing the isomerization process is given in Figure 3.

10.1021/jp014353b CCC: $22.00

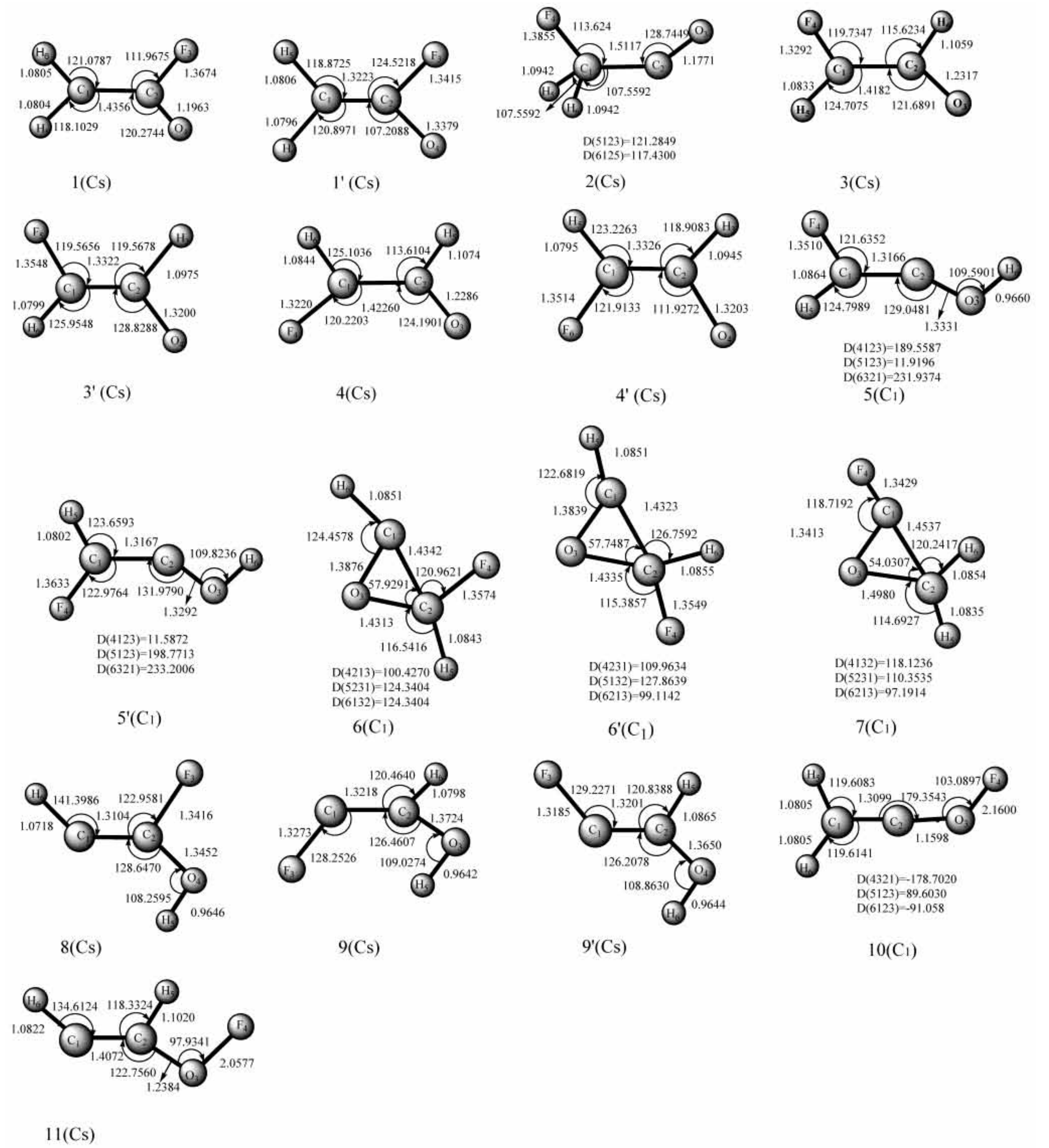

Figure 1. Optimized structures of C_2H_2FO isomers at the B3LYP/6-311G(d,p). Bond lengths are in angstroms and angles in degrees.

3.1. C_2H_2FO Species. In Figure 1, all of the possible structures are depicted, including seventeen minima structures with real frequencies. Among them, only isomer 1 (CH_2CFO) has been synthesized in experiment. From an analysis of laser induced single vibronic level fluorescence, some of the vibration frequencies were assigned for the ground-state $V_3 = 1724$ cm^{-1}-(C−O stretch), $V_5 = 1211$ cm^{-1}(C−F stretch), $V_6 = 906$ cm^{-1}(CH_2 rock), $V_7 = 847$ cm^{-1}(C−C stretch), $V_8 = 584$ cm^{-1}(CFCO bend), and $V_9 = 416$ cm^{-1}(CCO bond).[1] However, the corresponding frequencies are calculated to be 1747, 1234, 857, 768, 600, and 422 cm^{-1}, and this means that the calculated values are in good agreement with the experimental values. Isomer 1, 3, and 4 are all in the $^2A''$ electronic state, whereas isomer 1′, 3′, and 4′ are all with $^2A'$ state. For some of the isomers of the C_2H_3O radical, two electronic states, $^2A''$ and $^2A'$, are also in existence.[8−13] From a previous theoretical study by Baird et al., we can see the energy of $^2A''$ state is lower than that of $^2A'$ state.[17,18] The energy of 1 (CH_2CFO) with $^2A''$ is lower than that of $^2A'$ by 41.9 kcal/mol, the energy of isomer 3 (CFHCHO) with $^2A''$ is lower than that of $^2A'$ by 30.1 kcal/mol, the isomer 4 (CHFCHO) with $^2A''$ is lower than that of $^2A'$ by 28.7 kcal/mol. Because of the difference in electronic structure for the $^2A''$ structure, the σ lone pair electrons are on the oxygen atom, whereas for the $^2A'$ structure, the oxygen lone

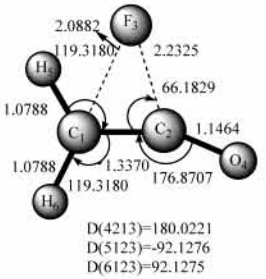

TS1/2(C1)

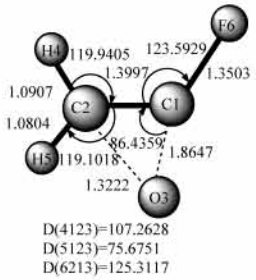

TS1/7(C1)

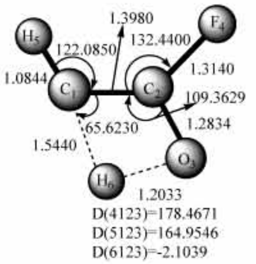

TS1/8(C1)

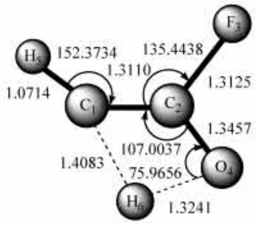

TS1/8*(Cs)

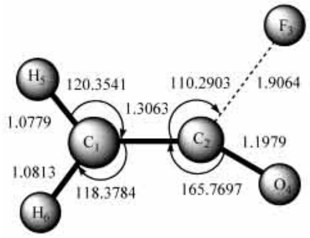

TS1/P1(Cs)

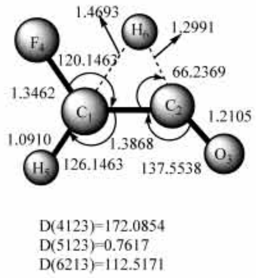

TS2/3(C1)

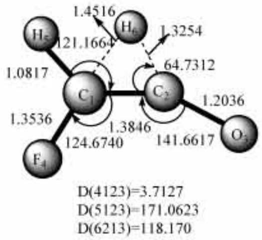

TS2/4(C1)

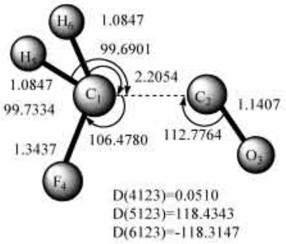

TS2/P2(C1)

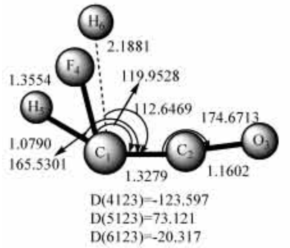

TS2/P3(C1)

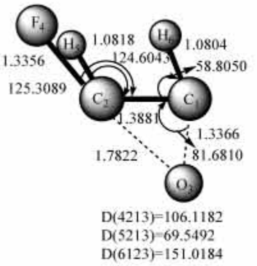

TS3/6(C1)

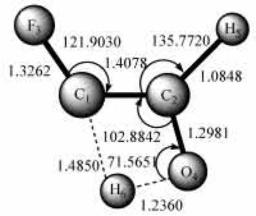

TS3/9'(Cs)

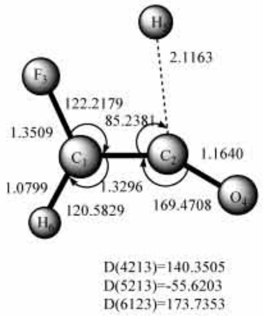

TS3/P3(C1)

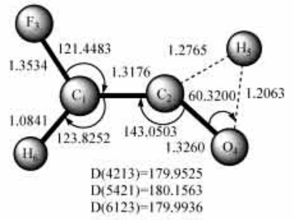

TS3'/5(C1)

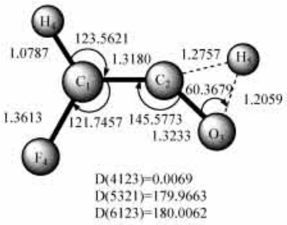

TS4/5'(C1)

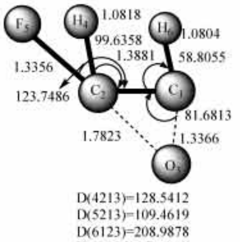

TS4/6'(C1)

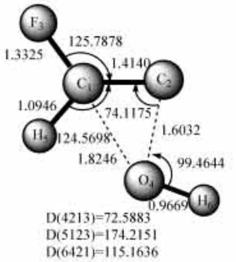

TS5/6'(C1)

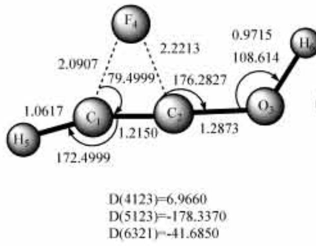

TS5/8*(C1)

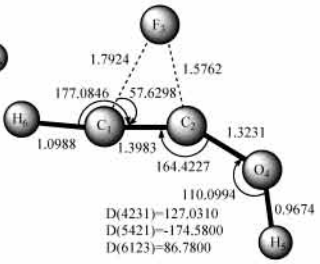

TS5/8(C1)

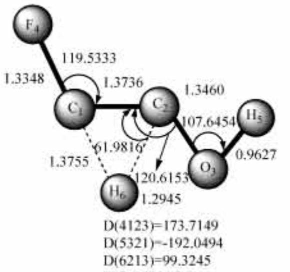

TS5/9'(C1)

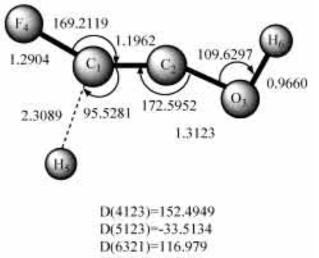

TS5/P6(C1)

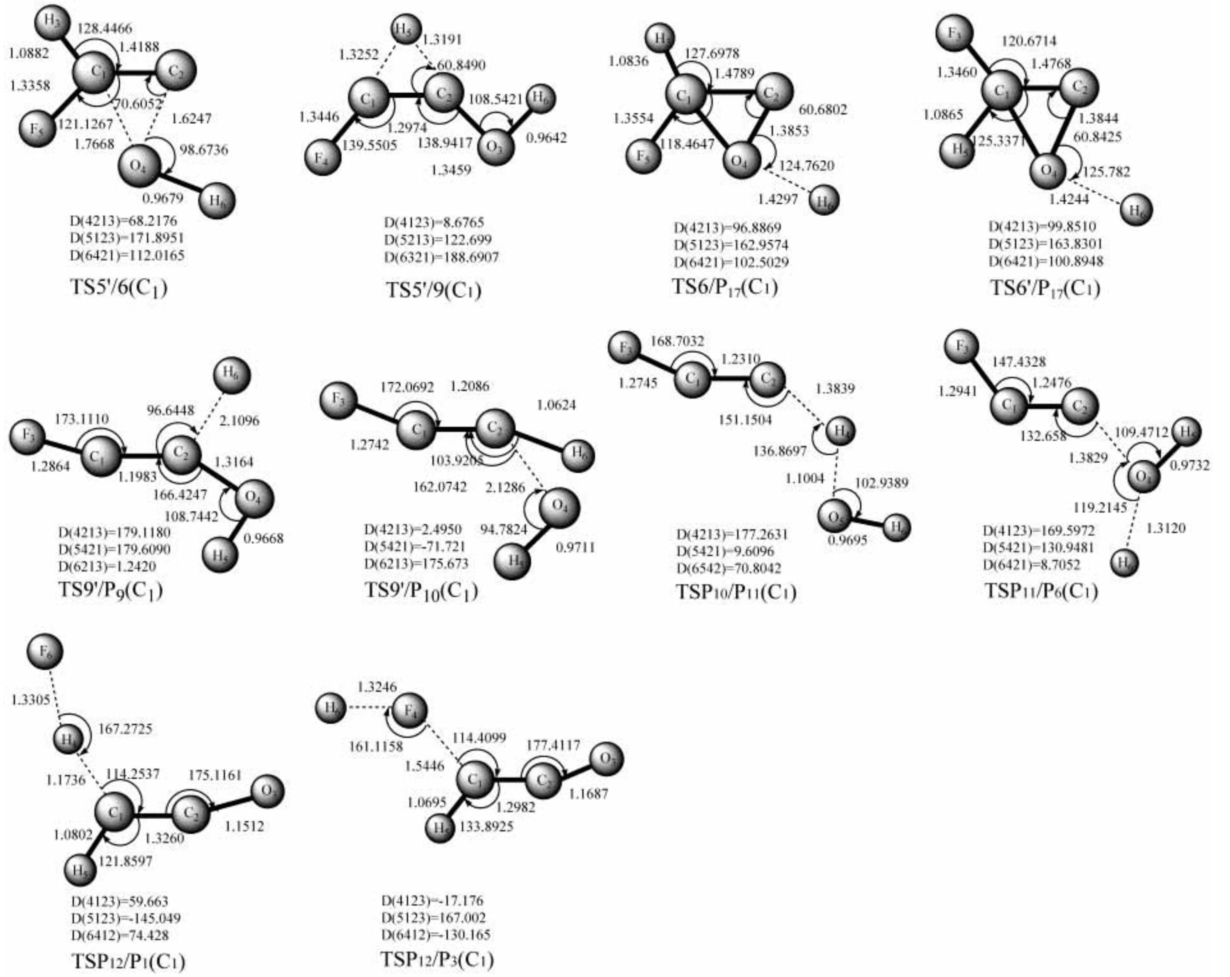

Figure 2. Optimized structures of C_2H_2FO transition states at the B3LYP/6-311G(d,p), Bond lengths are in angstroms and angles in degrees.

pair occupies a π orbital, and the unpaired electron occupies a σ orbital.[9] From Table 3, we can see that isomer 1 (CH_2CFO) is located in the lowest potential well in all of the species, and isomer 2 (CH_2FCO) is energetically higher than isomer 1 (CH_2CFO) by 15.5kcal/mol. However, for C_2H_3O species, the isomer CH_3CO is located in the lowest potential well.[19] The isomer CH_2CHO is higher than the former by 7.4kcal/mol at B3LYP/6-311G(d,p) level. Thus, due to the F atom substituent, the energy order has been changed, and this is attributed to conjugation of the carbonyl group in isomer 1 with substituent fluorine at the α-position, where fluorine acts as a π-donor.[16] This π-donor effect of fluorine has been confirmed by the experimental results and shows that it is very effective towards electron deficient carbon. The experimental study by Dolbier et al. indicates that β-fluorine substituents destabilize carbocations, whereas α-fluorines are stabilizing.[20] A similar conjugation effect has been studied by experiments which illustrate that halogen atoms adjacent to a carbocationic center inductively destabilize the cations due to their high electronegativity.[21] However, halogen atoms in trihalomethyl cations CX_3^+ can be stabilized by p−p interaction between the positively charged carbon atom and the nonbonded electron pairs on the adjacent halogens.[22] The isomers 5 (CHFCOH) and 5′ (CHFCOH) are a pair of trans- and cis- forms. They are active molecules and can be connected with many other isomers by interconversion transition states. Isomer 6 (CHOCFH), 6′ (CHOCHF), and 7 (CH_2OCF) are structures with three-membered ring consisted of C, C and O atom, and H, F atom, respectively, connected with the two C atoms.

Isomers 8 (CHCFOH), 9 (*trans*-CFCHOH), and 9′ (*cis*-CFCHOH) are planar structures. In addition, five other planar forms are found with imaginary frequencies and thus they are not minima isomers. Isomer 10 CH_2COF and 11 CHCHOF are special species, in that the F-atom is connected with O-atom, forming a long and thin bond. Their energies are very high, so they are easily dissociated.

3.2. Potential Energy Surface of C_2H_2FO. Let us turn our attention to the potential energy surface and to analyzing the kinetic stability of various C_2H_2FO isomers. The isomerization process of these C_2H_2FO species on potential energy surface is depicted in Figure 3. By means of the depth of potential well that the isomers reside in, we can then discuss their kinetic stability.

Isomers 1 (CH_2CFO) has four conversion channels, such as 1→2, 1→7, 1→8, 1→8*, and 1→P_1, their energy barriers are 50.6 kcal/mol, 69.0 kcal/mol, 77.3 kcal/mol, 88.4 kcal/mol, and 71.6 kcal/mol referred to TS1/2, TS1/7, TS1/8, TS1/8*, and TS1/P_1. Its F-elimination to P_1 ($F + CH_2{=}C{=}O$) needs 60.5 kcal/mol, and this suggests that there is a barrier of 11.1kcal/mol for the reaction of $F{+}CH_2{=}C{=}O$, which can make the reaction rate decrease. Then, both the conversion of isomer 1 and the dissociation need high energy, so the isomer 1 is stable. Isomer 2 converted to isomer 3 CFHCHO and 4 CHFCHO needs to overcome high barriers (48.6 kcal/mol and 56.8 kcal/mol respectively), whereas the energy barriers between TS2/3 and 3, as well as TS2/4 and 4 are 47.3 kcal/mol and 54.0 kcal/mol, respectively. However, the dissociation product P_2 ($CH_2F + CO$) needs to overcome 12.5 kcal/mol. Therefore, the kinetic stability

TABLE 1: Harmonic Vibrational Frequencies(cm^{-1}), Infrared Intensities (km/mol), Dipole Moment (debye), and Rotational Constant (GHz) of C_2H_2FO Structures at the B3LYP/6-311G(d,p) Level

species	frequencies (infrared intensity)	dipole moments	rotational constant
1 CH2CFO	320(0) 422(0) 600(15) 620(0) 768(50) 857(85) 1014(4) 1235(198) 1455(34) 1747(170) 3170(0) 3292(0)	3.0308	11.37250 10.75471 5.52749
1′ CH2CFO	405(3) 466(6) 635(0) 757(61) 793(31) 919(6) 930(64) 1261(99) 1402(2) 1719(282) 3175(13) 3275(1)	1.0332	12.02890 10.27843 5.54249
2 CH2FCO	219(3) 225(2) 680(29) 817(5) 888(5) 1032(134) 1265(0) 1363(11) 1448(13) 1950(98) 3045(10) 3095(7)	2.5103	22.65231 5.84386 22.91181
3 CFHCHO	242(13) 320(28) 565(0) 668(30) 959(1) 1125(85) 1220(58) 1319(9) 1455(89) 1579(38) 2947(72) 3211(3)	1.8625	56.08910 4.38932 4.07076
3′ CFHCHO	311(11) 348(5) 544(0) 741(3) 892(86) 1061(8) 1151(200) 1197(12) 1316(27) 1668(15) 3033(12) 3232(7)	0.2842	60.59372 4.23422 3.95766
4 CHFCHO	256(5) 364(0) 587(16) 796(58) 945(0) 960(0) 1241(54) 1398(25) 1462(26) 1579(61) 2927(85) 3196(11)	3.3492	23.52926 6.10058 4.84451
4′ CHFCHO	229(2) 514(0) 718(16) 757(43) 817(13) 1001(26) 1080(121) 1222(51) 1374(30) 1678(11) 3063(11) 3238(5)	2.4727	23.34466 5.87093 4.69116
5 FCHCOH	279(31) 294(1) 432(134) 551(1) 771(27) 1092(84) 1198(321) 1222(50) 1304(17) 1756(2) 3151(11) 3773(106)	2.5986	75.70300 4.00714 3.83916
5′ FCHCOH	211(9) 297(136) 469(42) 731(22) 807(20) 1003(62) 1115(193) 1220(121) 1347(35) 1765(46) 3230(3) 3776(109)	2.1367	26.04797 5.42695 4.53886
6 CHOCFH	437(15) 494(5) 789(51) 843(22) 969(50) 1046(119) 1103(42) 1178(29) 1325(12) 1448(91) 3162(5) 3177(14)	1.2880	22.62811 7.49214 6.70965
6′ CHOCFH	463(3) 507(2) 788(7) 814(80) 931(79) 1062(26) 1111(126) 1185(15) 1330(10) 1454(84) 3150(15) 3170(12)	2.2935	23.77304 7.37021 6.53342
7 CH2OCF	404(4) 509(4) 722(17) 889(81) 987(63) 1087(7) 1132(50) 1177(26) 1393(118) 1521(51) 3113(7) 3218(7)	2.1836	22.68991 7.52326 6.25380
8 CHCFOH	348(151) 422(18) 424(78) 538(4) 643(2) 757(35) 945(58) 1174(298) 1329(55) 1732(303) 3335(29) 3824(75)	0.7576	11.42027 10.88395 5.57283
9 CFCHOH	205(7) 325(52) 364(92) 749(13) 843(31) 1001(60) 1114(247) 1274(24) 1394(44) 1731(67) 3233(2) 3815(44)	0.3532	24.76965 5.65416 4.60336
9′ CFCHOH	233(23) 292(19) 411(105) 555(8) 744(13) 1079(14) 1190(351) 1261(21) 1368(68) 1746(0) 3153(7) 3808(40)	0.7173	75.95429 3.99510 22.64285
10 CH2COF	99(1) 208(0) 262(4) 439(2) 556(7) 650(111) 990(9) 1171(10) 1410(16) 2166(206) 3175(34) 3272(16)	3.7422	20.00389 4.14585 3.51918
11 CHCHOF	70(10) 172(5) 294(8) 476(0) 484(12) 853(25) 952(0) 1147(12) 1338(24) 1507(67) 2982(16) 3227(3)	4.8078	37.81943 3.82247 19.30150

of isomer 2 is governed by its dissociation to $CH_2F + CO$. It suggests that Isomer 2 is less stable than isomer 1. For the P_2, CH_2F radical and CO are important in combustion reaction, and the energy barrier between P_2 ($CH_2F + CO$) and Isomer 2 is low, 7.3kcal/mol, and thus, the reaction of $CH_2F + CO$ is possible and can produce a stable isomer.

Isomers 5 (CHFCOH) and 5′ (CHFCOH) are important molecules. They can be connected with many other isomers. Isomer 5 (CHFCOH) is connected with 3′ (CFHCHO), 6′ (CHOCHF), 8 (CHCFOH), 9′ (cis-CFCHOH), and P_6 (trans-FCCOH + H) by TS3′/5, TS5/6′, TS5/8, TS5/8*, TS5/9′, TS5/P_6. The energy barriers between these transition states and isomer 5 are 42.1 kcal/mol, 70.8 kcal/mol, 64.5 kcal/mol, 42.7 kcal/mol, 50.5 kcal/mol, and 65.9 kcal/mol, respectively. Isomer 5′ (CHFCOH) lies in a deeper potential well stabilized with the energy barrier of 42.1 kcal/mol by TS4/5′, 64.6 kcal/mol by TS5′/6, 56.4 kcal/mol by TS5′/9, whereas the energy barrier between TS4/5′ and isomer 4 is 72.0 kcal/mol, and that between TS5′/6 and isomer 6 is 65.1kcal/mol, as well as that between TS5′/9 and isomer 9 is 52.8 kcal/mol. Generally, the energy barriers conversion and dissociation are very high, which shows that isomer 4, 5, and 5′ are also stable. Isomers 6, 6′, and 7 are three-membered rings consisted of C, C, and O atom. They need to overcome barrier by 16.8 kcal/mol, 16.3 kcal/mol, and 20.1 kcal/mol for discharging ring to isomer 3, 4, and 1, respectively. P_{17} ($COCH_2 + F$) as cyclic isomer 6 and 6′ dissociating product need to overcome 22.6 kcal/mol and 20.9 kcal/mol by TS6/P_{17} and TS6′/P_{17}, respectively. So the three cyclic isomers are more stable than isomer 2, and less stable than isomer 1, 3, and 4.

Isomer 8 (CHCFOH), 9 (*trans*-CFCHOH), and 9′ (*cis*-CFCHOH) are planar structures. Isomer 8 is connected with isomer 1 and 5 though TS1/8, TS1/8*, TS5/8, TS5/8*, overcoming the energy barriers by 32.6 kcal/mol, 43.7 kcal/mol, 68.0 kcal/mol, and 46.2 kcal/mol, respectively. Isomer 9 needs to overcome the energy barrier by 52.8 kcal/mol to convert Isomer 5′. Isomer 9′ lies in a potential well with an barrier of 25.3 kcal/mol by TS3/9′, 46.6 kcal/mol by TS5/9′, 63.1 kcal/mol for the dissociation of 9′→P_9 (*cis*-FCCOH + H) via TS9′/P_9, and 44.3 kcal/mol for the dissociation 9′→P_{10} (FCCH + OH) via TS9′/P_{10}. Because FCCH and OH radical are important in combustion process, and the energy barrier from P_{10} (FCCH + OH) to isomer 9′ is low, 3.6 kcal/mol, the reaction of FCCH + OH is theoretically reasonable. From this analysis, it shows that isomers 8, 9, and 9′ are stable. Isomers 10 CH_2COF and 11 CHCHOF have high energies, and they are easily dissociated to the products P_1(CH_2CO+F) and P_{16}(CHCHO+F) by the barriers of 0.6 kcal/mol and 7.5 kcal/mol, respectively.

For the secondary reaction, four transition states are found, which are TSP_{10}/P_{11}, TSP_{11}/P_6, TSP_{12}/P_3, and TSP_{12}/P_1. We locate TSP_{10}/P_{11}, which is associated with the H-abstraction between FCCH and OH in P_{10} to give CFC and H_2O in P_{11}. TSP_{11}/P_6 is connected with CFC + H_2O and CFCOH + H in P_6. TSP_{12}/P_3 is connected with CHCO + HF in P_{12} and CFHCO + H in P_3. TSP_{12}/P_1 is located between CHCO + HF and CH_2CO + F. We can see the interesting structures of these transition states in Figure 2. Such processes may involve complex bond rearrangement. Because the energy of dissociation products except P_{12} are mostly very high, the barriers to dissociate are very high. Therefore, the secondary reaction cannot affect the kinetic stability of C_2H_2FO isomers.

From the above discussion, we can conclude that the isomers 1, 3, 4, 5, 5′, 8, 9, and 9′ have considerable kinetic stability,

TABLE 2: Harmonic Vibrational Frequencies (cm^{-1}), and Infrared Intensities(km/mol) of Interconversion Transition States between C_2H_2FO Isomers at the B3LYP/6-311G(d,p) Level

species	frequencies (infrared intensity)
TS1/2	150i (3) 242 (0) 352 (2) 435 (18) 447 (4) 639 (55) 998 (7) 1131 (4) 1398 (31) 2248 (611) 3188 (40) 3294 (23)
TS1/7	1422i (251) 375 (1) 511 (13) 723 (5) 901 (119) 1017 (21) 1038 (33) 1303 (31) 1365 (92) 1509 (52) 3092 (6) 3249 (1)
TS1/8	1926i (579) 282 (54) 490 (6) 600 (14) 708 (2) 968 (38) 1023 (102) 1082 (37) 1423 (367) 1470 (219) 2076(13) 3151(5)
TS1/8*	2072i (64) 488 (2) 607 (24) 608 (2) 661 (97) 846 (43) 1001 (69) 1248 (166) 1727 (230) 1919 (6) 3004 (384) 3341 (42)
TS1/P_1	399i(7) 282(4) 425(3) 436(0) 552(11) 668(108) 924(0) 1127(24) 1397(10) 2018(685) 3178(30) 3284(10)
TS2/3	1435i (7) 220 (6) 580 (18) 627 (32) 742 (59) 990 (120) 1174(159) 1192 (14) 1389 (23) 1801 (160) 1893 (62) 3226 (2)
TS2/4	1434i (7) 219 (6) 580 (18) 627 (31) 741 (59) 989 (122) 1174 (157) 1192 (14) 1389 (23) 1802 (159) 1893 (63) 3226 (2)
TS2/P_2	288i (9) 74 (4) 120 (1) 346 (2) 505 (0) 927 (4) 1153 (152) 1195 (6) 1478 (7) 2082 (266) 3102 (12) 3241 (12)
TS2/P_3	326i (89) 210 (10) 243 (13) 255 (14) 483 (3) 608 (26) 684 (9) 1033 (31) 1184 (60) 1400 (53) 2213 (569) 3238 (20)
TS3/6	656i (14) 371 (94) 493 (33) 571 (18) 884 (23) 1053 (182) 1115 (29) 1305 (31) 1344 (17) 1478 (135) 3212 (3) 3217 (1)
TS3/9′	1633i (388) 245 (0) 464 (8) 687 (6) 894 (7) 1121 (78) 1139 (39) 1198 (72) 1389 (192) 1436 (67) 2032 (21) 3192 (4)
TS3/P_3	550i (38) 155 (12) 288 (9) 386 (18) 471 (25) 518 (10) 656(5) 1026 (25) 1194 (72) 1407 (81) 2173 (359) 3230 (18)
TS3′/5	2093i (203) 163 (73) 269 (5) 325 (1) 557 (0) 655 (17) 1078 (39) 1175 (228) 1294 (96) 1724 (45) 2462 (63) 3179 (9)
TS4/5′	2010i (180) 118 (52) 205 (0) 413 (4) 720 (21) 727 (26) 980 (27) 1111 (229) 1349 (60) 1732 (69) 2467 (69) 3245 (3)
TS4/6′	656i (14) 371 (94) 493 (33) 571 (18) 884 (23) 1053 (182) 1115 (29) 1305 (31) 1344 (17) 1478 (135) 3212 (3) 3217 (1)
TS5/6′	749i (65) 346 (12) 431 (16) 591 (103) 647 (65) 953 (62) 1011 (44) 1041 (179) 1215 (92) 1400 (53) 3074 (15) 3793 (124)
TS5/8	220i (9) 84 (116) 269 (64) 372 (15) 435 (13) 563 (51) 710 (36) 1116 (134) 1241 (85) 2230 (218) 3483 (121) 3713 (113)
TS5/8*	358i (14) 352 (6) 422 (8) 528 (169) 677 (72) 741 (6) 823 (290) 1077 (42) 1236 (365) 1539 (100) 3019 (19) 375 (103)
TS5/9′	1064i (120) 324 (24) 342 (6) 481 (93) 583 (8) 1028 (79) 1144 (419) 1264 (34) 1295 (35) 1476 (18) 2090 (6) 3830 (154)
TS5/P_6	264i (66) 125 (106) 206 (17) 276 (11) 285 (1) 375 (7) 383 (17) 808 (3) 1246 (278) 1373 (162) 2464 (80) 3775 (104)
TS5′/6	462i (6) 451 (75) 499 (23) 600 (70) 646 (111) 945 (17) 1015 (85) 1042 (133) 1269 (115) 1402 (56) 3137 (12) 3785 (132)
TS5′/9	1642i (126) 188 (15) 385 (48) 452 (60) 621 (101) 625 (33) 893 (106) 1072 (427) 1283 (106) 1890 (101) 2199 (2) 3797 (106)
TS6/P_{17}	1654i (1988) 420 (2) 437 (15) 556 (7) 673 (5) 801 (36) 851 (82) 1069 (119) 1116 (16) 1270 (35) 1380 (43) 3184 (10)
TS6′/P_{17}	1566i (1460) 389 (5) 445 (0) 487 (12) 667 (2) 799 (35) 871 (102) 1093 (37) 1108 (118) 1284 (31) 1404 (58) 3150 (12)
TS9′/P_9	360i (61) 175 (85) 245 (2) 252 (48) 352 (0) 380 (25) 421 (27) 807 (5) 1243 (345) 1375 (124) 2448 (78) 3757 (104)
TS9′/P_{10}	282i (18) 97 (15) 201 (73) 354 (2) 421 (1) 625 (69) 672 (97) 713 (31) 1073 (100) 2237 (229) 3468 (97) 3746 (17)
TSP_{10}/P_{11}	1080i (166) 84 (2) 190 (79) 349 (10) 367 (2) 476 (16) 661 (99) 1072 (149) 1317 (55) 1702 (304) 2105 (841) 3775 (90)
TSP_{11}/P_6	1356i (2201) 243 (18) 275 (40) 336 (20) 422 (12) 651 (17) 793 (84) 930 (22) 1200 (305) 1265 (17) 2028 (75) 3660 (38)
TSP_{12}/P_3	1537i (3357) 144 (21) 207 (2) 248 (9) 358 (78) 550 (0) 610 (10) 873 (182) 1078 (5) 1309 (27) 2201 (855) 3351 (35)
TSP_{12}/P_1	1090i (24) 90 (3) 329 (32) 469 (13) 531 (2) 590 (44) 950 (19) 1150 (18) 1295 (55) 2100 (113) 2213 (640) 3240 (30)

TABLE 3: Total (a.u.) and Relative Energies in Parentheses (kcal/mol) of the C_2H_2FO Structures and Transition States at B3LYP/6-311G(d,p) and Single-Points CCSD(T)/6-311G(d,p) Levels

species	B3LYP/6-311G(d,p)	CCSD(T)/6-311G(d,p)
1 CH2CFO ($^2A''$)	−252.5049004(0.0)	−251.9245975(0.0)
1′ CH2CFO ($^2A'$)	−252.4393297(41.1)	−251.8577841(41.9)
2 CH2FCO	−252.4776605(17.1)	−251.9002212(15.5)
3 CFHCHO ($^2A''$)	−252.4812466(14.8)	−251.8978333(16.8)
3′ CFHCHO ($^2A'$)	−252.4331321(45.0)	−251.8498791(46.9)
4 CHFCHO ($^2A''$)	−252.478634(16.5)	−251.8954774(18.3)
4′ CHFCHO ($^2A'$)	−252.4343666(44.3)	−251.8496315(47.0)
5 FCHCOH	−252.4291443(47.5)	−251.8477197(48.2)
5′ FCHCOH	−252.4294988(47.3)	−251.8477197(48.2)
6 CHOCFH	−252.4263584(49.3)	−251.8484142(47.7)
6′ CHOCFH	−252.4255439(49.8)	−251.8477197(48.2)
7 CH2OCF	−252.4246166(50.4)	−251.8467441(48.9)
8 CHCFOH	−252.4333421(44.9)	−251.8533627(44.7)
9 CFCHOH	−252.4220128(52.0)	−251.8420988(51.8)
9′ CFCHOH	−252.4219303(52.1)	−251.8415348(52.1)
10 CH2COF	−252.4144967(56.7)	−251.8272987(61.1)
11 CHCHOF	−252.3011899(127.8)	−251.7137446(132.3)
TS1/2	−252.4400083(40.7)	−251.8439613(50.6)
TS1/7	−252.3980818(72.7)	−251.814669(69.0)
TS1/8	−252.3843961(75.6)	−251.8013875(77.3)
TS1/8*	−252.3683844(85.7)	−251.7836824(88.4)
TS1/P_1	−252.3994839(66.1)	−251.8105546(71.6)
TS2/3	−252.4096738(59.8)	−251.8224058(64.1)
TS2/4	−252.409638(59.8)	−251.8094327(72.3)
TS2/P_2	−252.4540221(31.9)	−251.8799242(28.0)
TS2/P_3	−252.3810709(77.7)	−251.7993961(78.6)
TS3/6	−252.4062150(61.9)	−251.8218303(64.5)
TS3/9′	−252.3860930(74.6)	−251.8012816(77.4)
TS3/P_3	−252.3789718(79.0)	−251.792691(79.9)
TS3′/5	−252.3658533(87.3)	−251.7807012(90.3)
TS4/5′	−252.3658602(87.2)	−251.7807027(90.3)
TS4/6′	−252.4062150(61.9)	−251.8218304(64.5)
TS5/6′	−252.3164577(118.2)	−251.7349045(119.0)
TS5/8	−252.3162882(118.4)	−251.729039(112.7)
TS5/8*	−252.3789434(79.0)	−251.7797294(90.9)
TS5/9′	−252.3532020(95.2)	−251.7702712(98.7)
TS5/P_6	−252.3216967(114.9)	−251.7428138(114.1)
TS5′/6	−252.3257118(112.4)	−251.7448193(112.8)
TS5′/9	−252.3422883(102.0)	−251.7578444(104.6)
TS6/P_{17}	−252.2838645(138.7)	−251.7034597(138.8)
TS6′/P_{17}	−252.2859186(137.4)	−251.7061116(137.1)
TS9′/P_9	−252.3216015(115.0)	−251.7409845(115.2)
TS9′/P_{10}	−252.3542170(94.6)	−251.7709413(96.4)
TSP_{10}/P_{11}	−252.3289791(110.4)	−251.7435591(113.6)
TSP_{11}/P_6	−252.2881258(136.0)	−251.7001588(140.8)
TSP_{12}/P_3	−252.3539715(94.7)	−251.7570841(105.1)
TSP_{12}/P_1	−252.4257042(49.7)	−251.8266479(61.5)
P_1: $CH_2CO + F$	−252.4015623(64.8)	−251.8282087(60.5)
P_2: $CH_2F + CO$	−252.4582461(29.3)	−251.8915962(20.7)
P_3: CFHCO + H	−252.3811902(77.6)	−251.8038146(75.8)
P_4: CHFCO +H	−252.3811900(77.6)	−251.8038131(75.8)
P_5: CHCOH +F	−252.3412922(102.7)	−251.7717334(95.9)
P_6: CFCOH +H	−252.32183221(114.9)	−251.7462213(111.9)
P_7: $COCH_2$ +F	−252.2955036(131.4)	−251.7329188(120.3)
P_8: CFHC +OH	−252.2723862(145.9)	−251.7013612(140.1)
P_9: CFCOH +H	−252.3218328(114.9)	−251.7462216(111.9)
P_{10}: CFCH +OH	−252.3500041(97.2)	−251.7766434(92.8)
P_{11}: CFC +H_2O	−252.3202605(115.9)	−251.7476121(111.1)
P_{12}: CHCO +HF	−252.4401366(40.6)	−251.8586954(39.1)
P_{13}: CFOCH +H	−252.3067597(124.3)	−251.7299410(122.1)
P_{14}: COCFH +H	−252.3059683(124.8)	−251.7392721(116.3)
P_{15}: CHOCF +H	−252.2949399(131.8)	−251.7235899(126.1)
P_{16}: CHCHO+F	−252.2730292(145.5)	−251.7018726(139.8)
P_{17}: COCHF+H	−252.3059676(124.8)	−251.7392731(116.3)

and their energy barriers are more than 30 kcal/mol. Isomer 2 has relatively lower kinetic stability. The three cyclic isomers 6, 6′, and 7 are less stable than the former, but more stable than the later. The other isomers such as isomers 1′, 3′, 4′, 10, and 11 are less stable than isomer 2 in kinetics. At present, only isomer 1 was synthesized experimentally, other stable isomers may be produced in the future from the reactions such as FCCH + OH and CH_2F +CO, etc.

3.3. Structural Properties of Relevant Species. Now let us examine the spin densities of these isomers. For Isomer 1 ($CH_2CF{=}O$) with $^2A''$, the spin densities of C, C, F, O, H, and H are 0.937,−0.092, 0.004, 0.233, −0.042, and −0.041, respectively. The length of C−C is 1.4356 Å, the unpaired electron mainly positioned at the first C atom. Isomer 1′ ($CH_2{=}CFO$) with $^2A'$, the length of C=C is 1.3223 Å, the spin densities

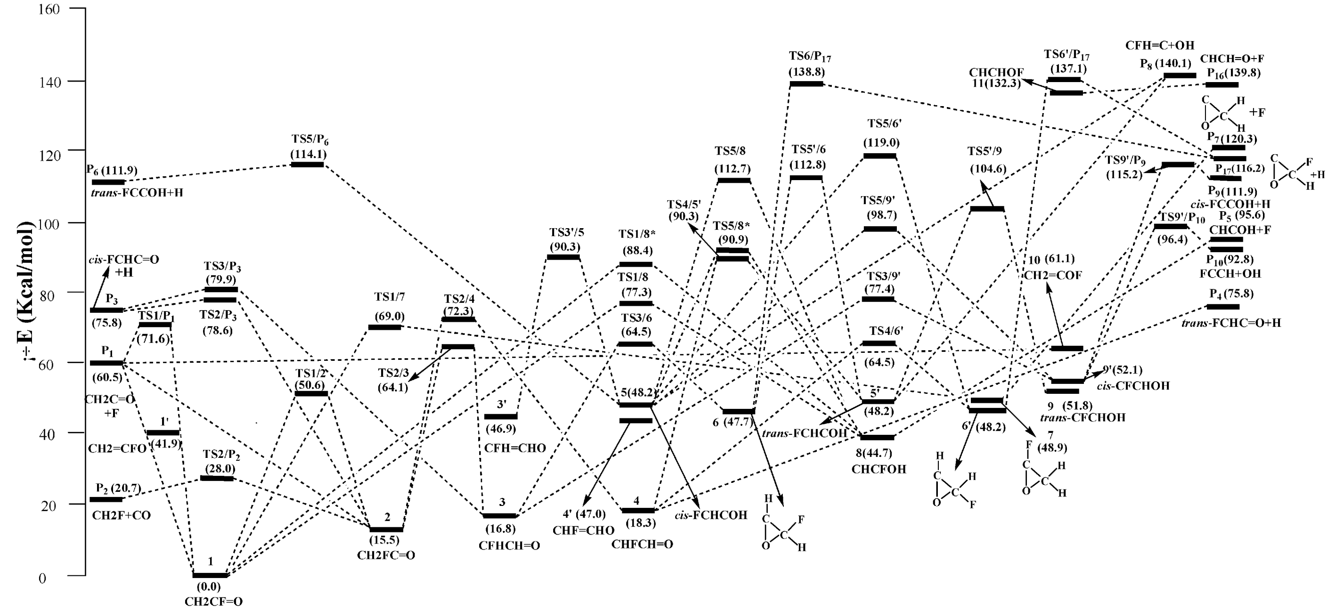

Figure 3. Schematic potential energy surface of C_2H_2FO at the CCSD(T)/6-311G(d.p) level.

(−0.053, −0.025, 0.030, 1.033, 0.011, and 0.004 for C, C, F, O, H, and H, respectively) illustrate the lone electron positioned at the O atom neighboring to F atom. Such valence structures are confirmed by the nature bond order (NBO) analysis. Similarly, isomer 3 with $^2A''$, the spin densities of C, C, F, O, H, and H are 0.705, −0.105, 0.358, 0.078, −0.036, and −0.001, respectively, which suggests a valence structure CFHCH═O, isomer 3′ (CFH═CHO) with $^2A'$, the spin densities of each atom are 0.015, −0.038, 0.095, 0.920, 0.001, and 0.006, respectively. Because isomers 3 and 4 are trans- and cis- forms, their spin densities are similar. Isomer 4 (CHFCH═O) with $^2A''$, the spin densities of each atom are 0.076, −0.099, 0.352, 0.080, −0.003, and −0.004, respectively, illustrating that the lone electron mainly positioned at the first C atom neighboring to F atom. The spin densities of each atom in 4′ (CHF═CHO) with $^2A'$ are 0.013,−0.04, 0.095, 0.926, 0.006, and 0.001, respectively. According to NBO analysis, the unpaired electron positioned at the O atom neighboring to F atom.

On the other hand, among C_2H_3O radical, for isomer CH_3-CO, the spin densities of C, C, O, H, H, and H are 0.076, 0.618, 0.254, 0.052, −0.002, and −0.002, respectively, suggesting the lone electron positioned between the second C atom and O atom. However, Isomer CH_2FCO, the spin densities of C, C, F, O, H, and H are 0.099, 0.579, 0.290, 0.031, 0.000, and 0.000, respectively, illustrating that the unpaired electron positioned between the second C atom and F atom. Because the charges of the F atom are more than that of the H atom, when the F atom is substituted, the lone electron is located near the F atom. For the spin densities of most isomers, the lone electron is located neighboring to the F atom. If two F atoms are substituted, then the unpaired atom may be positioned between the two F atoms. This problem will be discussed in future paper.

4. Conclusion

The kinetic stability of every isomer are studied by the potential energy surface of C_2H_2FO radical using CCSD(T)/6-311G(d,p) method. It indicates that isomers of 1, 3, 4, 5, 5′, 8, 9, and 9′ are stable, and the energy barriers are more than 30 kcal/mol. Isomer 2 has relatively lower kinetic stability. The three cyclic isomers, 6, 6′, and 7, are less stable than the former, but more stable than the latter. The other isomers, such as isomers 1′, 3′, 4′, 10, and 11, are less stable than isomer 2 with regard to kinetics. Only isomer 1 was produced experimentally, and the calculated frequencies are in good agreement with experimental values, so we conjecture that other stable isomers may be produced by the experimental methods in the future, for example coming from the reactions such as FCCH + OH, CH_2F + CO, and so forth. Compared with the analogue C_2H_3O radical isomers, the energy order is changed, and the reasons may be due to conjugation of the carbonyl group in isomer 1 CH_2CFO with substituent fluorine at the α-position.

Acknowledgment. This work was supported by the National Natural Science Foundation of China (Nos. 29892168, 20073014, and 20103003), Doctor Foundation of Educational Ministry, Foundation for University Key Teacher by the Ministry of Education and Key Term of Science and Technology by the Ministry of Education of China.

References and Notes

(1) Furubayashi, M.; Bridier, I.; Inomata, S.; Washida, N. *J. Chem. Phys.* **1997**, *106*, 6302.

(2) Solomon, S. *Rev. Geophys.* **1988**, *26*, 131.

(3) Vaida, V. Solomn, S.; Richard, E. C.; Ruhl, E, Jefferson, A. *Nature* **1989**, *342*, 405.

(4) U. S. Congress. Offece of Technology Assessment. *Complex Cleanup: The Environmental Legacy of Nuclear Weapons Production OTA-O-484;* U. S. Government Printing Office: Washington, DC, 1991; p 150.

(5) (a) Buss, R. J.; Baseman, R. J.; He, G.; Lee, Y. T. *J. Photochem.* **1981**, *17*, 389. (b) Kleinermanns, K.; Luntz, A. C. *J. Phys. Chem.* **1981**, *85*, 1966. (c) Schmidt, V.; Zhu, G. Y.; Becker, K. H.; Fink, E. H. *3rd Europ. Sym. On Physicochemical Behavior of Atomspheric Pollutants* **1984**. Ispra (Varese). (d) Lorenz, K.; Zellner, R. Ber. Bunseges. *Phys. Chem.* **1984**, *88*, 1228. (e) Endo, Y.; Tsuchtya, E.; Yamada, C.; Hirota, E.; Koda, S. *J. Chem. Phys.* **1986**, *85*, 4446. (f) Schmoltner, A. M.; Chu, P. M.; Brudzynski, R. J.; Lee, Y. T. *J. Chem. Phys.* **1989**, *91*, 6926.

(6) Baldwin, R. R.; Walker, R. W. *Symp. (Int) Combust. Proc.* **1981**, *18*, 819.

(7) Finlayson-Pitts, B. J.; Pitts, J. N., Jr. *Atomspheric Chemistry: Fundamentals and Experimental Techniques*; John Wiley and Sons: New York, 1986, pp 425−431.

(8) Hunziker, H. E.; Kneppe, H.; Wendt, H. R. *J. Photochem.* **1981**, *17*, 377.

(9) Dupuis, M.; Wendoloski, J. J.; Lester, W. A., Jr., *J. Chem. Phys.* **1982**, *76*, 488.

(10) Jacox, M. E. *Chem. Phys.* **1982**, *69*, 407.

(11) Heaven, M.; DiMauro, L.; Miller, T. A. *Chem. Phys. Lett.* **1983**, *95*, 347.

(12) DiMauro, L. F.; Heaven, M.; Miller, T. A. *J. Chem. Phys.* **1984**, *81*, 2339.

(13) Huyser, E. S.; Feller, D.; Bordon, W. T.; Davidson, E. R. *J. Am. Chem. Soc*. **1982**, *104*, 2956.

(14) Inomata, S.; Furubayashi, M.; Imamura, T.; Washida, N. *J. Chem. Phys*. **1999**, *111*, 6356.

(15) Srivatsva, A.; Arunan, E.;. Manke II, G and Setser, D. W.; Sumathi, R. *J. Phys. Chem. A*.**1998**, *102*, 6412.

(16) Sung, K. S.; Thomas T. Tidwell. *J. Org. Chem*. **1998**, *63*, 9690.

(17) Baird, N. C.; Gupta, R. R.; Taylor, K. F. *J. Am. Chem. Soc*. **1979**, *101*, 4531.

(18) Baird, N. C.; Taylor, K. F. *Can. J. Chem*. **1980**, *58*, 733.

(19) Ding, Y. H.; Zhang, C.; Li, Z. S.; Huang, X. R.; Sun, C. C. *J. Phys. Chem. A.* **2001**, *105*, 8206.

(20) Tian, Feng.; Battiste, M. A.; Dolbier, W. R., Jr. *Organic Lett.* **1999**, 1, 193.

(21) Olah, G. A.; Rasul, G.; Heiliger, L.; Surya Prakash G. K. *J. Am. Chem. Soc.* **1996**, *118*, 3580.

(22) *22.Corboium Ions*; Olah, G. A., Schleyer. P. v. R., Eds.; Wiley-Interscience: New York, 1976, 2135.